Histol Histopathol (1997) 12: 447-457

Histology and Histopathology

Field emission SEM, conventional TEM and HVTEM study of submandibular gland in prenatal and postnatal aging mouse

I. Watanabe[1], C. Jin[2] and T. Nagata[2]

[1]Department of Anatomy, Institute of Biomedical Sciences, University of Sao Paulo, Brazil and

[2]Department of Anatomy and Cell Biology, Shinshu University, School of Medicine, Matsumoto, Japan

Summary. The development of acinar and ductal cells of the mouse submandibular gland was studied using field emission SEM, conventional TEM and HVTEM methods. The specimens, at 15 and 18 days of gestation and 1, 3, 7, 14, 21, 30, 90 and 180 postnatal days were fixed in 2.5% glutaraldehyde solution in 0.1M sodium phosphate buffer (pH 7.3). At 15 and 18 days of gestation, the structure of mouse submandibular gland contains acinar and ductal cells in proliferation. The cytoplasmic organelles such as mitochondria, granular endoplasmic reticulum and Golgi apparatuses are scattered in the cytoplasm. At 18 prenatal days only several acinar cells present immature secretory granules in the apical portion. In this stage the acinar and ductal cells are enveloped by bundles of fine collagen fibrils disposed in several directions. There are also numerous capillaries located closely to the acinar cell membranes. In the aging stages of 1, 3, 7, 14, 21, and 30 postnatal days, the histo-differentiation of acinar, intercalated and ductal cell components are observed. At newborn day one the cytoplasmic organelles start to place themselves around the nucleus. Several immature secretory granules are observed at day one, however, they increase in the aging days. At postnatal day 30, the cytoplasms of acinar and ductal cells are filled with a large number of secretory granules of different sizes. The stacks of granular endoplasmic reticulum and Golgi apparatus and some vesicles and free ribossomes are noted. The intercellular membranes are attached by desmosomes and cytoplasmic interdigitations. The luminal surface shows several small projections of microvilli. An electron-dense line of basement membranes followed by fine collagen fibrils are recognized. Delicate capillaries are found in the outer surface of acinar cells. At postnatal day 90 and 180 the acinar, intercalated and striated ductal cells reveal numerous secretory granules in the apical portion. The acinar cells showed basal nuclei and the parallel arrangement of granular endoplasmic reticulum. The mitochondria are located at the base of ductal cells showing a typical pattern of cristae. In these stages the intercellular digitations of cytoplasmic protrusions and desmosomes are also noted. The cytoplasm of myoepithelial cells are seen along the cell membranes. The spongy-like structures constituting the basement membrane are followed by bundles of fine collagen fibers.

Key words: Submandibular gland, aging mouse, acinar cell, field emission SEM

Offprint requests to: Prof. Dr. I. Watanabe, Department of Anatomy, Institute of Biomedical Sciences, University of Sao Paulo, Cep 05508-900 Cidade Universitária, Sao Paulo, Brazil

Introduction

Several studies of salivary glands have demonstrated the different features of morphology, histochemistry and ultrastructure of acinar and ductal cells, including TEM and SEM aspects (Parks, 1952; Scott and Pease, 1959; Shackleford, 1963; Cowley and Shackleford, 1970; Ichikawa and Ichikawa, 1977; Boshell and Wilborn, 1983; Espinal et al., 1983; 1985; Nagato and Tandler, 1986; Watanabe et al., 1989, 1992a,b, 1994). On the other hand, the postnatal development and changes of rat submandibular glands were reported by Jacob and Leeson (1959), Tamarin and Sreebny (1965), Dvorak (1969), Sashima (1986), Scott et al. (1986), and Sashima et al. (1988). As for the mouse salivary gland several papers are available at present referring essentially to morphological characteristics, and histoenzymological and radioautographic studies (Srinivasan and Chang, 1979; Denny et al., 1988, 1990; Jayasingle et al., 1990; Chen et al.,1995; Accili et al., 1996).

The purpose of this study was to demonstrate the ultrastructural organization of the mouse submandibular gland during the development from 15 days of gestation to 180 postnatal days, using conventional transmission electron microscopy (TEM), high voltage transmission

electron microscopy (HVTEM) and field emission scanning electron microscopy (FESEM).

Material and methods

Sixty-two fetuses, young and adult mice in 10 groups from 15 and 18 prenatal days, and 1, 3, 7, 14, 21, 30, 90 and 180 postnatal days were used in the present study. All the animals were puchased from S.L.C. (Shizuoka Laboratory Center), Inc., Hamamatsu, Japan.

They were sacrificed in each stage under ethyl ether anesthesia and the submandibular glands were excised carefully, and fixed in a solution containing 2.5% glutaraldehyde in 0.1M sodium phosphate buffer (at pH 7.3) for 12 h at 4 ºC.

Transmission electron microscopy

The submandibular glands at 15 and 18 prenatal days, and 1, 3, 7, 14, 21, 30, 90 and 180 days, were fixed in a solution containing 2.5% glutaraldehyde in 0.1M sodium phosphate buffer at 4 ºC (pH 7.3). Then, the tissues were rinsed in phosphate buffer for 15 min, and postfixed in 1% buffered osmium tetroxide for 2h at 4 ºC.

The dehydration was done at room temperature with an increasing series of ethanol, and they were embedded in epoxy resin (Epok 812, Oken, Tokyo, Japan). Thick sections, about 3 μm, were cut on a Porter-Blum type MT-2B ultramicrotome (DuPont-Sorvall, Newtown, USA) and stained with 2% toluidine blue solution for light microscopy, in order to examine the general views of structures. Then, the thick sections ranging from 1-2 μm, and thin sections, about 0.1 μm, were cut with a diamond knife on the Porter-Blum MT-2B ultramicrotome. The grids were counterstained with uranyl acetate and lead citrate and examined in a conventional medium voltage Hitachi H-700 transmission electron microscope at 100-200 kV or a JEOL, JEM-4000EX high voltage transmission electron microscope at 400kV in the Department of Anatomy and Cell Biology at Shinshu University School of Medicine.

Field emission scanning electron microscope (FESEM)

The mice submandibular glands at 15 and 18 prenatal days, and 1, 3, 7, 14, 21, 30, 90 and 180 days were fixed in a solution containing 2.5% glutaraldehyde in 0.1M sodium phosphate buffer (at pH 7.3) for 12 h at 4 ºC. Then, the tissues were rinsed in distilled water for 6 h at 4 ºC, and immersed successively in 12.5%, 25% and 50% dimethylsulfoxide (DMSO) solution for 60 min each. They were freeze-cracked in 50% DMSO, using liquid nitrogen with an Eiko TF-1 apparatus, according to the technique described by Tanaka (1981, 1989). After cracking, the pieces were placed in a 50% DMSO solution followed by a rinse in distilled water overnight at 4 ºC. The specimens were postfixed in buffered 1% osmium tetroxide for 2h at 4 ºC, and immersed in 1% tannic acid solution for 1h at room temperature (Murakami, 1974).

The samples were dehydrated in an increasing series of ethanol and dried in a JEOL JCPD-5 apparatus, using liquid CO_2. The dried specimens were mounted with carbon double surface tape on QTY, JEOL Datum lamina, coated with Quick Cool Coater SC-701 MC (Sanyo Denshi CO. Ltd, Tokyo, Japan) and examined in a JEOL JSM-6000F field emission scanning electron microscope at 10 and 15 kV, in the Department of Anatomy and Cell Biology at Shinshu University School of Medicine.

Results

The scanning electron microscopic observations of the mouse submandibular gland at the 15th day of gestation revealed several groupings of acinar formations, and intercalated and striated ducts (Fig. 1). These structures contained numerous epithelial cells in development, and capillaries in adjacent areas. The acinar portions and intercalated ducts were formed by pyramidal cells containing spherical nuclei in basal portions. The granular endoplasmic reticulum was located at random as were the few slender mitochondria and free ribosomes (Figs. 2, 3). Small vesicles were commonly seen in the cytoplasm near to the Golgi

Fig. 1. FESEM image of a fetal day 15 mouse submandibular gland. DMSO freeze-cracked specimen showing the terminal acinar portions, and intercalated and striated ductal cells in development. x 400

Fig. 2. HVTEM image of a fetal day 15 mouse, revealing the cytoplasm of four acinar cells and the lumen. The nucleus and cell organelles are observed. x 10,000

Fig. 3. TEM image of a fetal day 15 mouse a high magnification, showing the nucleus, granular endoplasmic reticulum, free ribosomes and Golgi apparatus with small vesicles. x 48,000

Fig. 4. TEM image of a fetal day 18 mouse submandibular gland. General view of acinar cells showing large nuclei at the basal portion, and the organelles scattered into the cytoplasm. Several immature secretory granules are noted. x 6,000

Fig. 5. TEM image of a fetal day 18 mouse a high magnification, revealing the mitochondria, stacks of Golgi apparatus, granular endoplasmic reticulum and free ribosomes. x 30,000

Figs. 6 and 7. HVTEM stero-pair images of a fetal day 18 mouse. Note immature secretory granules, lumen, desmosomes and cytoplasmic organelles in three-dimensional characteristics. X 4,000

apparatus. In the cytoplasm of acinar cells in this stage no secretory granules were observed. Between the acinar cell membranes intercellular digitations and desmosomes were seen (Fig. 2).

At the 18th day of gestation the mouse submandibular gland presented acinar and ductal cells

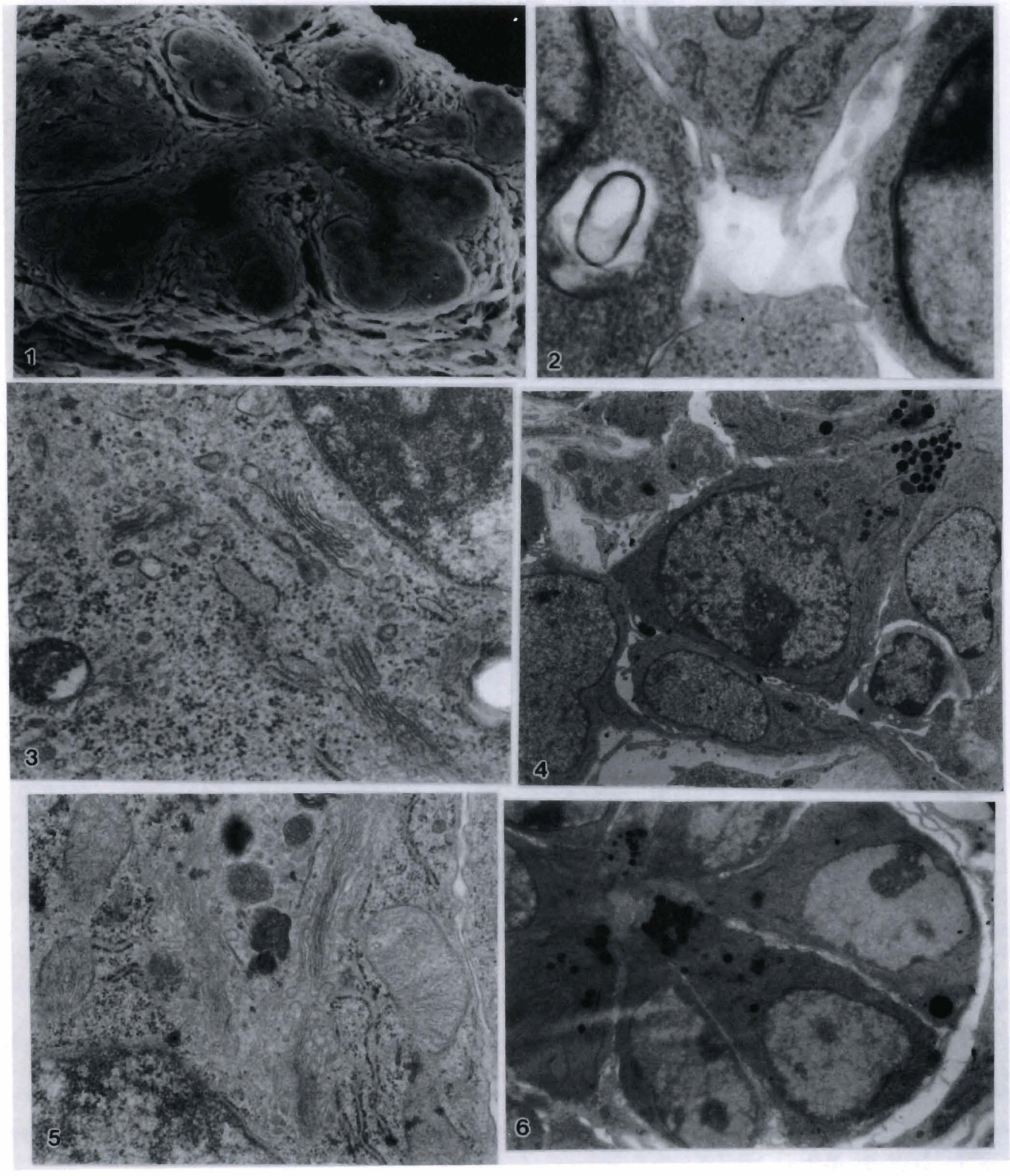

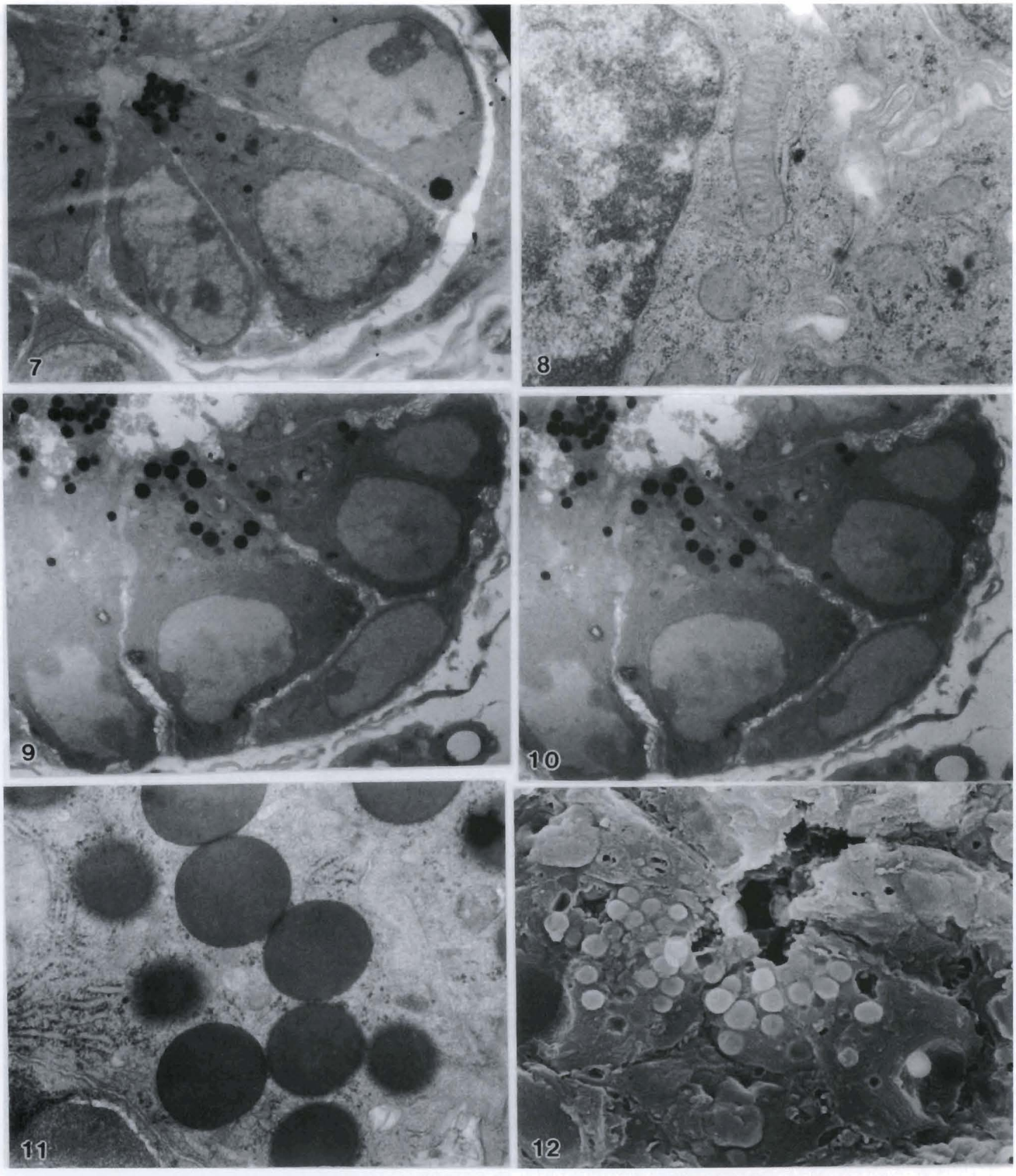

Figs. 6 and 7. HVTEM stero-pair images of a fetal day 18 mouse. Note immature secretory granules, lumen, desmosomes and cytoplasmic organelles in three-dimensional characteristics. x 4,000

Fig. 8. TEM image of a day 1 newborn mouse. The mitochondria with their characteristic pattern of cristae, granular endoplasmic reticulum, desmosomes and cytoplasmic protrusions are observed. x 27,000

Figs. 9 and 10. HVTEM stereo-pair images of a day 1 newborn mouse. Several acinar cells and the lumen containing small microvilli are noted in 3D aspects. x 4,000

Fig. 11. TEM image of a day 1 newborn mouse. At high magnification, the granular endoplasmic reticulum and secretory granules are seen. x 30,000

Fig. 12. FESEM image of a postnatal day 3 mouse submandibular gland. DMSO freeze-cracked specimen showing numerous acinar cells and striated ducts. x 10,000

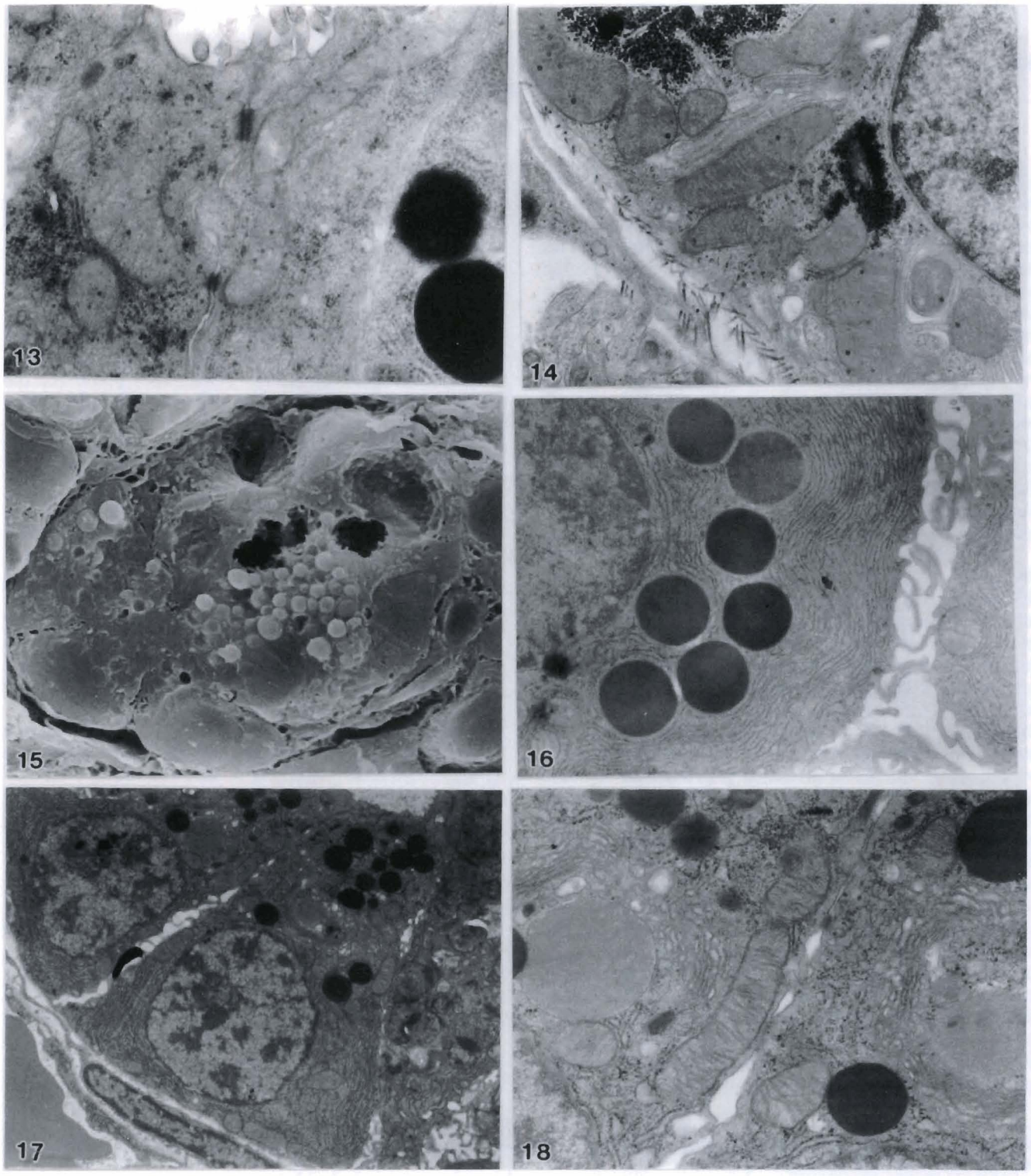

Fig. 13. TEM image of a day 3 postnatal mouse. The surface of the lumen contains numerous microvilli (small arrows), and the desmosomes between the acinar cell membranes are noted (large arrows). x 30,000

Fig. 14. TEM image of a day 3 postnatal mouse. Shows the cytoplasm of striated ductal cell revealing the mitochondria, glycogen granules and the cytoplasmic infoldings of cell membrane. x 18,000

Fig. 15. FESEM image of a postnatal day 7 mouse submandibular gland. DMSO freeze-cracked specimen revealing acinar terminal portions. Several immature secretory granules are noted. x 7,000

Fig. 16. TEM image of a day 7 postnatal mouse. The nucleus, granular endoplasmic reticulum and secretory granules are identified. Between the acinar cell membranes several cytoplasmic interdigitations are present. x 15,000

Fig. 17. TEM image of a day 14 postnatal mouse. The acinar cell showing the organelles and several secretory granules at the apical portion are noted. x 7,000

Fig. 18. TEM image of a day 14 postnatal mouse. At high magnification, the stacks of Golgi apparatus, mitochondria, granular endoplasmic reticulum and secretory granules are shown. x 24,000

which were polygonal in shape, and contained round nuclei at the basal portion (Fig. 4). The acinar cells in developing stage revealed only several immature secretory granules in the apical portion (Fig. 4). The slender mitochondria and granular endoplasmic reticulum were scattered in the cytoplasmic matrix. The Golgi apparatus was oriented longitudinally near the nuclei, presenting parallel stacks (Fig. 5). The membranes of acinar cells were attached, specially near the lumina, with several desmosomes. The luminal surface showed cytoplasmic projections forming small microvilli. The stereo-pair images by HVTEM (Figs. 6, 7) demonstrated the acinar cells with the nuclei located at the base and the intracellular components in three-dimensional characteristics. The basement membrane was noted as an electron-dense line followed by a network of fine collagen fibers.

The freeze-cracked specimens of one day after birth observed by field emission SEM revealed the characteristics of acinar and ductal cells of mouse submandibular gland. The acinar portions corresponding to the terminal tubules showed the acinar cells with immature secretory granules of different diameters. The lumen was clearly noted with small projections of microvilli. The fractured specimens of ducts showed a flat surface with large nuclei in the central portion and the lumina showing several microvilli. The mitochondria were oval or elongated in shape, revealing an internal pattern of membranes or cristae, and were scattered in the cytoplasm (Fig. 8). Only a few secretory granules measuring from 0.5 to 1.2 μm in diameter were present at the apical portion. The lumen was seen as an irregular shape and presented some microvilli (Figs. 9, 10). The Golgi apparatus and granular endoplasmic reticulum were more organized at this stage (Fig. 11). Between the two acinar cells several desmosomes and cytoplasmic intercellular digitations existed. The HVTEM stereo-pair images revealed the arrangement of granular endoplasmic reticulum, located mainly around the nucleus at the basal portion in three-dimensional aspects (Figs. 9, 10). The basement membrane of acinar cells was continuous, as an electron-dense line on the cell membrane.

The submandibular gland of a mouse at 3 days after birth, showed many acinar and ductal cells which were more developed than those observed in anterior stages. The DMSO freeze-cracked specimens, as examined by field emission SEM, revealed the different stages of cells. In the SEM images, the lumen of endpieces was clearly observed, presenting numerous microvilli oriented in several directions (Fig. 12). In the SEM and TEM images, the pyramidal acinar cells possessed the nuclei at the basal portion and the immature secretory granules in the apical region (Fig. 12). In the cytoplasm of acinar cells the arrangement of granular endoplasmic reticulum was noted in parallel stacks. The lumen of acinar cell and striated ductal cells observed in HVTEM permitted us to identify numerous microvilli disposed in three-dimensional images. At this stage the slender mitochondria were scattered in the cytoplasm (Fig. 13) there were interdigitations of cytoplasmic protrusions between the cell membrane and the desmosomes were near to the lumen (Fig. 13). In the horizontal section of intercalated and striated ducts, polygonal cells were also revealed. In this segment the nuclei were located at the base and the mitochondria were found between the infoldings of cell membranes (Fig. 14).

The submandibular gland of a day 7 postnatal animal presented the acinar terminal portions as round in shape (Fig. 15) and the segments of intercalated and striated ducts. The acinar cells showed a pyramidal form and demonstrated several secretory granules presenting different diameters. The HVTEM stereo-pair images showed the intracellular components such as secretory granules accumulated near to the lumen, the arrangement of granular endoplasmic reticulum, and the nuclei being at the basal portion. The mitochondria were slender and the stacks of Golgi apparatus were noted (Fig. 16). The lumen of acinar cells presented an irregular surface revealing several microvilli. The intercellular membranes near to the lumen showed several desmosomes and gap junction areas. The interdigitations were numerous at the base of acinar cells.

In the SEM samples of the freeze-cracked surfaces

Fig. 19. TEM image of a day 14 postnatal mouse. General view of striated ductal cells showing the nucleus, arrangement of mitochondria and infoldings of cell membrane (small arrows). x 7,000

Fig. 20. FESEM image of a postnatal day 21 mouse submandibular gland. DMSO freeze-cracked specimen revealing the terminal portion. The lumen and several secretory granules are also seen. x 3,000

Fig. 21. TEM image of a day 21 postnatal mouse . Cytoplasm of two acinar cells showing the mitochondria and the stacks of granular endoplasmic reticulum . Numerous cytoplasmic interdigitations (small arrows), basement membrane (large arrow) and adjacent fine collagen fibers are seen. x 12,000

Fig. 22. TEM image of a day 21 postnatal mouse. The granular endoplasmic reticulum, mitochondria, desmosomes (small arrow), and the secretory granules are observed. x 12,000

Fig. 23. FESEM image of a day 30 postnatal mouse. DMSO freeze-cracked surface of striated ductal cells revealing numerous secretory granules. x 2,000

Fig. 24. TEM image of a day 30 postnatal mouse. The striated ductal cells showing the nuclei, mitochondria at the base, and secretory granules near to the lumen are shown. x 3,600

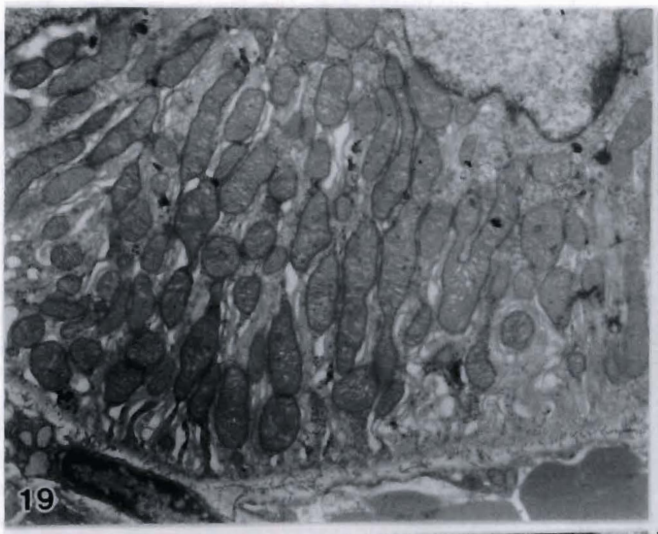
19

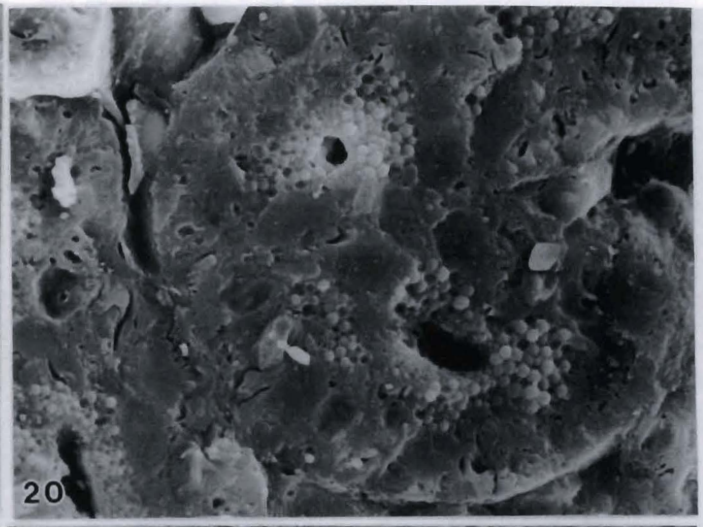
20

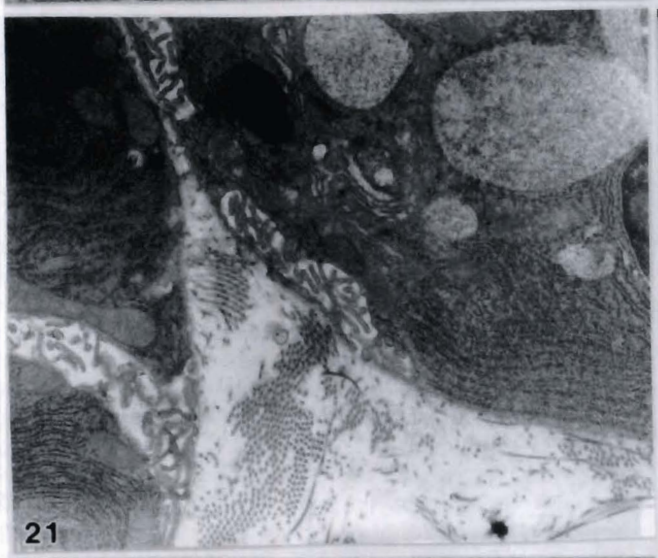
21

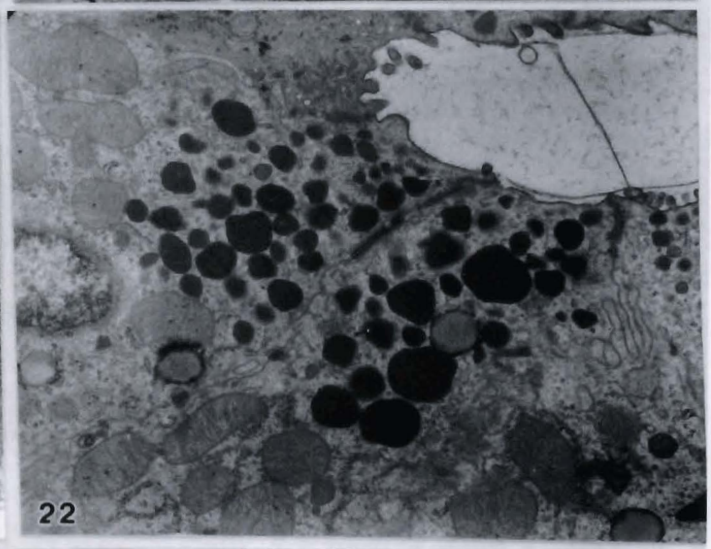
22

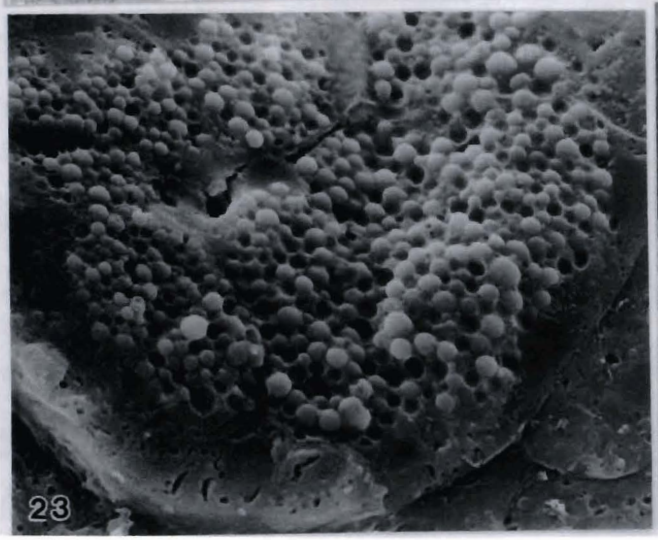
23

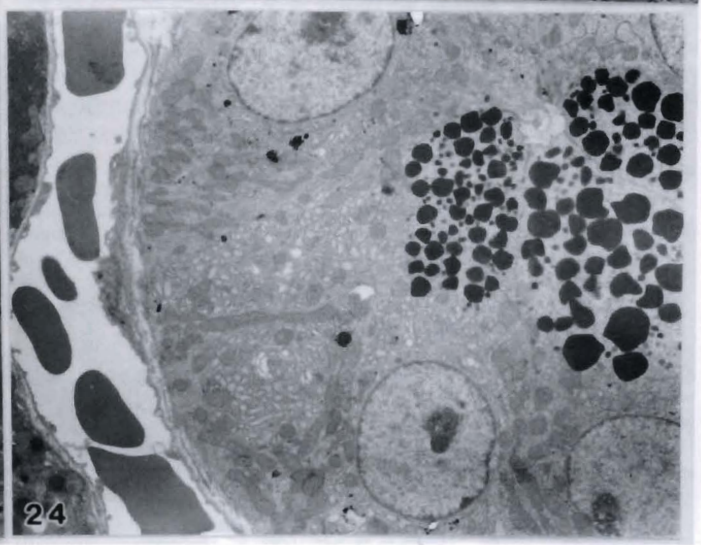
24

of mouse submandibular gland at 14 postnatal days the acinar endpieces and striated ductal cells presented a pyramidal form and contained several secretory granules. In the HVTEM and TEM images, the terminal tubules forming acinar cells showed a large nuclei at the base (Fig. 17). Several groupings of secretory granules with different diameters were noted at the apical region. The arrangement of granular endoplasmic reticulum was located around the nucleus and slender mitochondria intermingled (Fig. 18). At high magnification the stacks of Golgi apparatus are observed showing the characteristic pattern of their cristae. The attatchment of intercellular membranes was made by desmosomes. On the other hand, the striated ductal cells were revealed the disposition of numerous mitochondria at the base and the nuclei in the central portion (Fig. 19). Between the mitochondria, the infoldings of cell membranes were clearly seen (Fig. 19). These often showed their long axes arranged in parallel to the long axes of the cells. In the cytoplasm small granules of glycogen and free ribosomes were detected (Fig. 19). The basement membrane appeared as an electron-dense line, contacting the adjacent fine collagen fibrils. The bundles of collagen fibers were disposed in several directions.

The SEM observations of the mouse submandibular gland at 21 postnatal days showed acinar and striated ductal cells presenting a variable number of secretory granules (Fig. 20). The nucleus was located at the base, and the secretory granules were close to the luminal surface (Fig. 20). At the periphery of the cells there were numerous small capillaries. TEM and HVTEM stereo-pair images confirmed the localization of nuclei and the arrangement of the stacks of granular endoplasmic reticulum in three-dimensional characteristics. The stacks were disposed in parallel and the mitochondria were also scattered in the cytoplasm (Fig. 22). Few cytoplasm protrusions forming microvilli were observed at the surface of the lumen. Between the acinar cells there were desmosomes and interdigitations of cytoplasmic protrusions (Fig. 21). At this stage the secretory granules were observed in the apical portion. At the periphery of the cell membrane, the bundles of fine collagen fibrils disposed in several directions were noted (Fig. 21).

After 30 postnatal days the mouse submandibular gland, the acinar terminal portions and striated ducts presented a large number of secretory granules (Fig. 23). In SEM images the acinar cells showed a pyramidal form, containing the nuclei at the base. At high magnification different sizes of secretory granules, which measured from 0.3 to 1.2 μm in diameter were clearly observed. In the TEM and HVTEM observations the presence of acinar and ductal intracellular components were shown. The acinar cells presented a large number of secretory granules closely located to the lumen. There were desmosomes between the cell membrane and some microvilli were evident on the surface of lumen. At high magnification the parallel arrangement of granular endoplasmic reticulum, mitochondria, Golgi apparatuses and secretory granules was observed. The cytoplasmic interdigitations were numerous at this stage. The pyramidal cells of striated ducts showed a large nuclei in the central portion, and the mitochondria had an elongated form, presenting their characteristic internal pattern (Fig. 24). Many of them measured about 300nm in diameter. Some mitochondria were very long and were separated by infoldings of the basal cell membranes.

The mouse submandibular gland at 90 postnatal days presented more differentiated ultrastructural characteristics when compared to other previous stages. The freeze-cracked surface examined by field emission scanning electron microscopy demonstrated a large number of secretory granules in all acinar and striated ductal cells (Fig. 25). The secretory granules were occupied almost all extensions of apical region and the size and form of these granules are variable. In TEM and HVTEM observations of the mouse submandibular gland revealed that the acinar cells possessed a large nucleus and organelles at the base, and numerous secretory granules in the apical region. The cytoplasm of acinar cells at this stage presented different sizes of secretory granules, granular endoplasmic reticulum, Golgi apparatuses and mitochondria (Fig. 26). These cells were enveloped by cytoplasmic laminae of myoepithelial cells which were attached to the surface. The surface of the basement membrane of acinar and myoepithelial cells was constituted spongy-like

Fig. 25. FESEM image of a day 90 postnatal mouse. DMSO freeze-cracked surface of striated duct revealing the pyramidal cells with numerous secretory granules. x 2,800

Fig. 26. TEM image of a day 90 postnatal mouse. The cytoplasm of acinar cell containing large amount of secretory granules, cytoplasmic extensions of myoepithelial cells (arrows) are observed. x 2,400

Fig. 27. FESEM image of a day 90 postnatal mouse. The basement membrane with sponge-like structures and fine collagen fibrils are observed. x 50,000

Fig. 28. FESEM image of a day 180 postnatal mouse. DMSO freeze-cracked surface of striated duct revealing pyramidal cells with numerous secretory granules. x 2,800

Fig. 29 . HVTEM image of a day 180 postnatal mouse. The stacks of granular endoplasmic reticulum, secretory granules and mitochondria are seen. x 18,000

Fig. 30. FESEM image of a day 180 postnatal mouse. At high magnification, note the network of fine collagen fibers. x 80,000

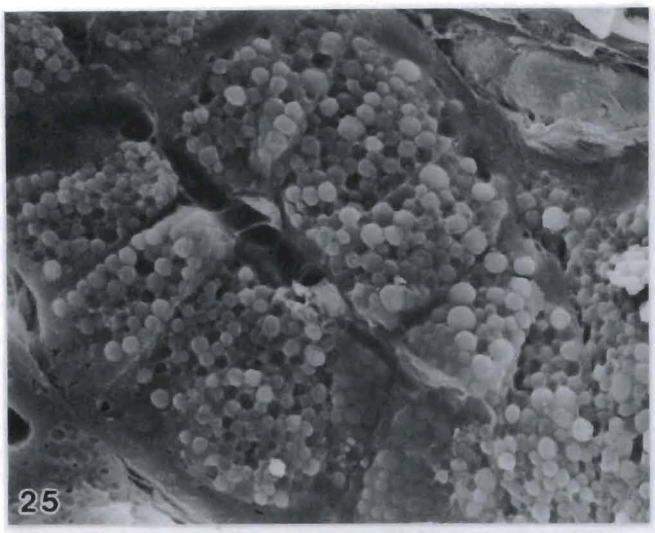
25

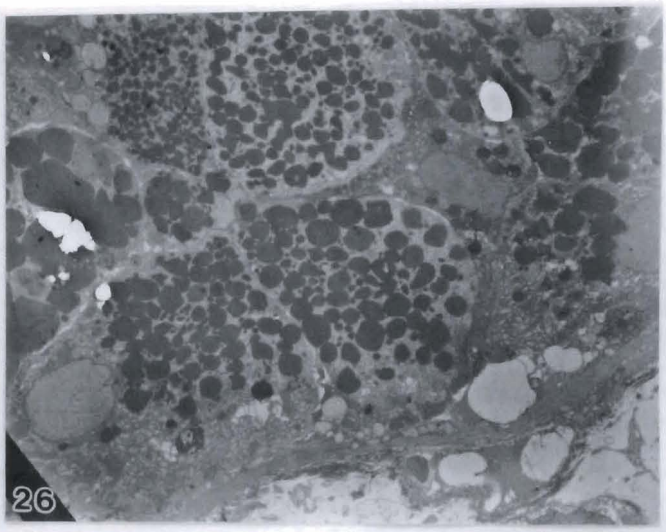
26


27

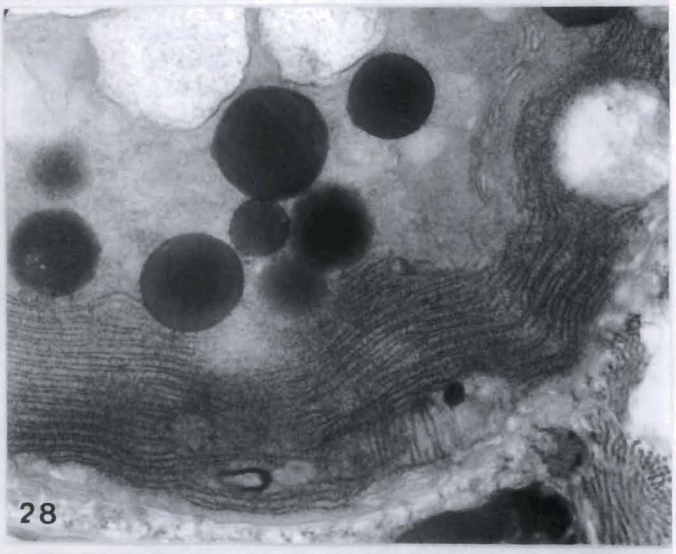
28

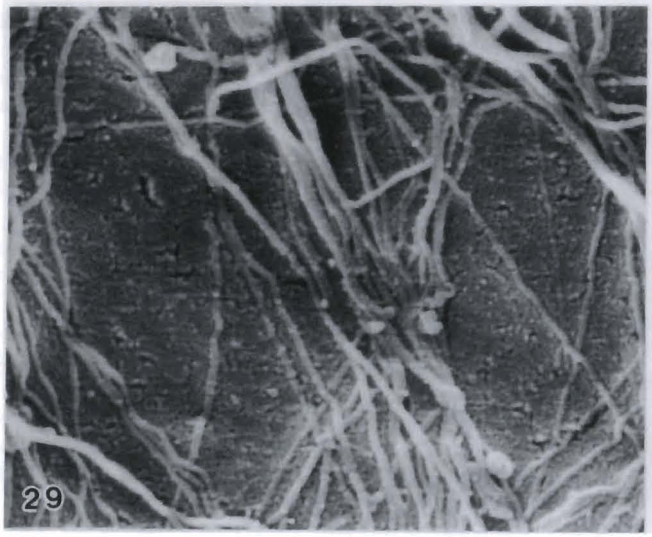
29

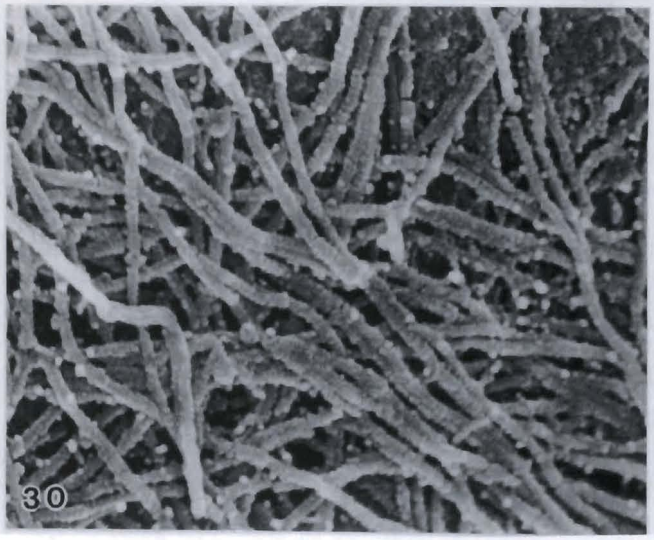
30

structures covered by fine collagen fibrils in three-dimensional configuration (Fig. 27).

At 180 days of age the mouse submandibular gland examined by FESEM showed numerous secretory granules in the acinar and ductal cells (Fig. 28). The cell organelles were concentrated in the basal portion and the secretory granules were noted in the apical region. The HVTEM images clearly revealed the stacks of granular endoplasmic reticulum around the nucleus, and Golgi apparatus and secretory granules located at random near to the apical region (Fig. 29). In the external surface of acinar cell membrane the myoepithelial cell cytoplasm was observed (Fig. 29). The spongy-like structures of basement membrane and associated network of collagen fibers were noted in the three-dimensional images (Fig. 30).

Discussion

Our data demonstrated the characteristics of the acinar, intercalated and striated ductal cells of the mouse submandibular gland during development in prenatal and postnatal aging stages. During these stages we could observe the proliferation and histo-differentiation of cells structures.

The data confirmed that at 15 days of gestation, the epithelial cells forming several groupings constitute the acinar endpieces, and intercalated and striated ductal cells. In this stage the profiles of granular endoplasmic reticulum are scattered in the cytoplasm as well as Golgi apparatuses and a few slender mitochondria are observed. In this stage did not observe the secretory granules in the cytoplasm. However, the acinar cells at 18 days of gestation demonstrated cell organelles located at random, revealing several secretory granules in the apical portion. The HVTEM stereo-pair images of thick sections demonstrated the characteristics of these cellular components in three-dimensional aspects.

Our findings also confirm that in aging animals starting at 1, 3, 7, 14, 21, and 30 postnatal days, the acinar and ductal cells are developed successively following these ages. The histo-differentiation presenting more organized intracellular components in the acinar and ductal cells are clearly demonstrated in the TEM images, such as granular endoplasmic reticulum, mitochondria, Golgi apparatus, and the increasing number of secretory granules. On the other hand, at postnatal day 30 the acinar and striated ductal cells revealed well developed organelles and were characterized by a great number of secretory granules of different diameters. These observations are similar to those observed by TEM images in rat submandibular glands by Tamarin and Sreebny (1965), Leeson and Jacob (1959), and Jacob and Leeson (1959), and in SEM images by Watanabe et al. (1989).

At 90 and 180 postnatal days, the acinar and the striated ductal cells observed by SEM and TEM images demonstrated the nuclei in the basal portion and the cell organelles in the apical portion containing a large number of secretory granules. In our observations at each stage of 30, 90 and 180 days, the SEM images of freeze-cracked specimens revealed a great number of secretory granules indicating that in these periods the secretion is continued intensively.

With respect to the lumen of acinar cells and the striated ducts it may be emphasized that the presence of microvilli became more numerous according to age. Cellular junctions are present between the membranes of acinar cells which are characterized by desmosomes of different sizes. Finally, we believe that these data are important to clarify the sequence of development of acinar and ductal cells of mouse submandibular salivary glands in the prenatal and postnatal stages.

Acknowledgements. This study was supported in part by a Grant-in-Aid for Scientific Research from the Ministry of Education, Science and Culture of Japan during Professor I. Watanabe was visiting Professor at the Department of Anatomy and Cell Biology at Shinshu University, Japan.

References

Accili D., Gabrielli M.G., Menghi G. and Materazzi G. (1996). Histoenzymological detection of sialic acids in the rodent salivary glands. Histol. Histopathol. 11, 647-658.

Boshel J.L. and Wilborn W.H. (1983). Differences in the ultrastructure of the submandibular glands of baboon and rhesus monkeys by the use of different fixatives. Cell Tissue Res. 231, 655-661.

Chen S., Gao F., Kotani A. and Nagata T. (1995). Age-related change of male mouse submandibular gland: a morphometric and radioautographic study. Cell. Mol. Biol. 41,117-124.

Cowley L.H. and Shackleford J.M. (1970). An ultrastructural study of the submandibular glands of the squirrel monkey *Saimiri Sciureus*. J. Morphol. 132, 117-136.

Denny P.A., Pimprapaiporn W., Kim M.S. and Denny P.A. (1988). Quantitation and localization of acinar cell-specific mucin in submandibular glands of mice during postnatal development. Cell Tissue Res. 251, 381-386.

Denny P.C., Chai Y., Pimprapaiporn W. and Denny P.A. (1990). Three-dimensional reconstruction adult female mouse submandibular gland secretory structures. Anat. Rec. 226, 489-500 .

Dvorak M. (1969). The secretoy cells of the submandibular gland in the perinatal period of development in the rat. Z. Zellforsch. 99, 346-356.

Espinal E.G., Ubios A.M. and Cabrini R.L. (1983). Freeze-fractured surface of salivary glands of rat observed by scanning electron microscopy. Acta Anat. 117, 15-20.

Espinal E.G., Ubios A.M., Pardier P. and Cabrini R.L. (1985). Scanning electron microscopy of human submandibular gland. Acta Anat. 122, 25-28.

Ichikawa M. and Ichikawa A. (1977). Light and electron microscopic histochemistry of serous secretory in the salivary glandular cells of the Mongolian gerbil (*Mongolian Meridianus*) and rhesus monkey (*Macaca irus*). Anat. Rec. 189, 125-140.

Jacob F. and Leeson C.R. (1959). The postnatal development of the rat submaxillary gland. J. Anat. 93, 201-216.

Jayasingle N.R., Cope G.H. and Jacob S. (1990). Morphometric studies

on the development and sexual dimorphism of the submandibular gland of the mouse. J. Anat. 172, 115-127.

Leeson C.E.R. and Jacob F. (1959). An electron microscopic study of the rat submaxillary gland during its postnatal development and in the adult. J. Anat. 93, 287-295.

Murakami T. (1974). A revised tannic osmium method for noncoated electron microscope specimens. Arch. Histol. Jpn. 36, 198-193.

Nagato T. and Tandler B. (1986). Ultrastructure of the submandibular gland in two species of macaques. Acta Anat. 126, 255-262.

Parks H.E. (1952). Morphological study of the extrusion of secretory materials by the parotid glands of mouse and rat. J. Ultrastruct. Res. 6, 449-465.

Sashima M. (1986). Age-related changes of rat submandibular gland: a morphometric and ultrastructural study. J. Oral Pathol. 15, 507-512.

Sashima M., Hatakeyama S., Satoh M. and Suzuki A. (1988). Age-related changes of the granular intercalated ductal cells of male submandibular gland. Archs. Oral Biol. 33, 71-73.

Scott B.L. and Pease D.C. (1959). Electron microscopy of the salivary and lacrimal glands of the rat. Am. J. Anat. 104, 115-161.

Scott J., Bonder L. and Baum B.J. (1986). Assessment age related changes in the submandibular and sublingual glands of the rat using stereological analysis. Archs. Oral Biol. 31, 69-71.

Shackleford J.M. (1963). Histochemical comparison of mucous secretory in rodent, carnivore, ungulate and primate major salivary glands. Ann. NY Acad. Sci. 106, 572.

Srinivasan R. and Chang W.W.L. (1979). The postnatal development of the submandibular gland of the mouse. Cell Tissue Res. 198, 363-371.

Tamarin A. and Sreebny L.M. (1965). The rat submaxillary salivary glands. I. Correlative study by light and electron microscopy. J. Morphol. 117, 295-352.

Tanaka K. (1981). Demonstration of intracellular structures by high resolution scanning electron microscopy. Scann. Electr. Microsc. 2, 1-8.

Tanaka K. (1989). High resolution scanning electron microscopy of cell. Biol. Cell 65, 89-98.

Watanabe I., Ogawa K. and Yamada E. (1989). Rabbit parotid gland acini as revealed by scanning electron microscopy. Cienc. Cult. 41, 284-287.

Watanabe I., Ogawa K., Koriyama Y. and Yamada E. (1992a). Rat submandibular gland: fracture surface observed by scanning electron microscope. Rev. Cien. Biomed. 13, 89-93.

Watanabe I., Koriyama Y. and Yamada E. (1992b). High resolution scanning electron microscopic study of mouse submandibular salivary gland. Acta Anat. 143, 59-66.

Watanabe I., Yamada E., Kawano Y.K. and Ogawa K. (1994). Scanning electron microscopy of acinar cells of rat submandibular salivary glands. Braz. J. Med. Biol. Res. 27, 2197-2206.

Accepted November 11, 1996